Time-Resolved Analysis of Film Cooling Effects Under Pulsating Inflow Conditions

Alexander Heinrich(✉), Markus Herbig, and Dieter Peitsch

Chair for Aero Engines, Institute for Aeronautics and Astronautics, Technische Universität Berlin, Berlin, Germany
alexander.heinrich@tu-berlin.de

Abstract. The development of modern gas turbines requires higher turbine inlet temperatures for an increase in thermal efficiency. With a change to a pressure gain combustion concept to increase the efficiency significantly, more challenges for the cooling of the first turbine stages must be overcome. For this purpose an array of 777 fan-shaped cooling holes on a flat plate are exposed to a series of different pulsating inflow conditions. Varying the amplitude up to 100% to the mean differential pressure, the film cooling performance is analyzed and evaluated. Adjusting the pulsating frequencies from 1 Hz–5 Hz further allows to gain a comprehensive understanding of the influence of the main parameters affecting the cooling film development. The experimental data recorded with an infrared thermography system reveals a strong impact of the pulsating inflow conditions on the adiabatic film cooling effectiveness.

Keywords: Film cooling · Pressure gain combustion · Turbine

η	Adiabatic film cooling effectiveness
ρ_∞	Main flow air density
ρ_c	Secondary flow air density
CRC	Collaborative Research Centre
DR	Density ratio
f_p	Pulse frequency
l_{ax}	Axial position of cooling hole
M	Blowing ratio
NGV	Nozzle guide vane
Re	Reynolds number
T_∞	Main flow air temperature
T_{aw}	Adiabatic surface temperature
T_c	Secondary flow air temperature
V_∞	Main flow velocity
V_c	Secondary flow air density

R. King and D. Peitsch (Eds.): AFCC 2021, NNFM 152, pp. 153–168, 2022.
https://doi.org/10.1007/978-3-030-90727-3_10

1 Introduction

In order to significantly increase overall gas turbine efficiency by up to 10%, a change from a classical constant pressure to a pressure gain combustion might be the necessary adjustment to realise the aforementioned goal [10,19]. Recent research efforts by the Collaborative Research Centre (CRC) 1029 have thoroughly examined the feasibility of such an approach and also highlighted the challenges for the turbomachinery components in terms of unsteady combustion and flow dynamics. The influence of these boundary conditions on the integrity and performance of the turbine have been subject to numerous experimental investigations.

A change from a constant pressure to a pressure gain combustion has a direct impact on the cooling concepts of the downstream turbine. In contrast to the classical combustion method, the new combustion concept imposes strong temporal variations in the total pressure, in temperature and in an incidence variation of the incoming flow. Especially the Nozzle Guide Vane (NGV) of the first turbine stage is poised to withstand those new boundary conditions. In order to gain a comprehensive understanding of the impact on the cooling concepts the turbine research efforts have been clustered. Whereas this paper concentrates on the impact on the film cooling formation, accompanying research by Heinrich et al. [7] and Topalovic et al. [20] has looked at the turbine performance with varying incidence angle due to the pulsating inflow conditions and means to homogenize these distortions.

The basic idea of film cooling is to act as a heat sink and to provide a thin cooling boundary layer around a body to protect it from the hot main gas flow. For this purpose cooling air is fed through holes from the inside of a blade to the outside, where it is supposed to unite and build an uniform cooling film, shielding the blade material from the hot main gas flow. Recent developments have seen a shift from classical cylindrical holes towards so-called fan-shaped or laidback cooling holes. Cylindrical holes have the disadvantage of producing a lift-off of the cooling jet from the blade surface at higher blowing ratios. The resulting jets rather resemble the desired characteristics for flow control applications and do not favor the formation of a uniform cooling film [1,3]. Further research has then analysed the aforementioned fan-shaped or laidback coolings holes. As Auf dem Kampe et al. have been reporting, the benefit of these configurations is the expanded exit which decreases the jet entrainment velocity thus resulting in a laterally wide spread cooling film [8]. Various researchers have analysed the effect of adjusting the outlet geometry for their desired applications and made recommendations which, however, cannot easily be transferred to general applications. Schroeder and Thole have researched the various available geometries and published a condensed geometry which serves as a baseline for adopting different experimental and numerical investigations [14–18]. This thoroughly examined open-access geometry, called 777 geometry, is intended to be used by other researchers and also serves as a baseline for these research efforts.

Little research was carried out, investigating the direct influence of the pulsating inflow conditions on the film cooling effects. Some conclusions can be drawn from the work of Heidmann et al. [6] and Womack et al. [21]. Heidmann looked at the impact of wake passing on the film cooling effectiveness and observed a

decrease in effectiveness for all analyzed blowing ratios. Womack followed the same question, using a flat plate geometry and noted that for blowing ratios which experienced a slight lift-off, the wake can actually promote reattachment in the near hole region. However a strong disturbance of the film cooling jets was the overall perception. Bakhtiari and Schiffer [2] have, as one of the few researchers, numerically analyzed the influence of transient inflow conditions originating from a pressure gain combustion on the film cooling effects. For their numerical investigations they used cylindrical holes which were exposed to a sinusoidal oscillation of the pressure amplitude. They report that in the case of pulsating inflow, the film cooling effectiveness decreases and the heat transfer coefficient rises.

2 Experimental Facility

The experimental film cooling measurements are conducted in a low-speed wind tunnel at the Chair of Aero Engines at the Technische Universität Berlin. Operated by a radial compressor, that is sucking the air through the measurement section, a main flow velocity (V_∞) up to 40 m/s can be realized. Through the periodic blocking of the flow path a periodic unsteady main flow can be produced. This concept of generating flow instabilities was proved by several investigations before [4,5,9]. An integrated air heater for the main flow as well as a heat exchanger for the secondary air flow provides the necessary density ratio to determine the resulting film cooling effectiveness. A full overview of the setup is given in Fig. 1.

For a detailed acquisition of a surface temperature field an infrared thermography system is used. Optical access is provided by a 5 mm thick Germanium window with a diameter of 75 mm which is placed above the flat plate. The camera lens is positioned almost flush mounted on the Germanium window to reduce any backlight interference. In addition, a special anti-reflection coating is chosen to allow for sufficient transmission for thermal imaging applications in the wavelength range of 8.000–12.000 nm.

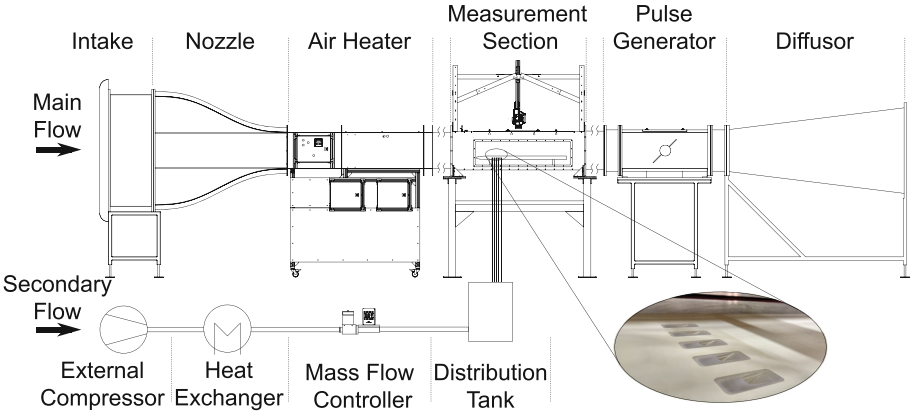

Fig. 1. Scheme of the low-speed wind tunnel

The main flow is sucked into the nozzle from ambient. Downstream, a 40 kW air heater enables maximum main flow temperatures of 323 K. From an aerodynamic point of view the air heater causes unwanted disturbances in the velocity and temperature distribution. However, a homogeneous temperature field can be reached using a turbulence grid that improves the temperature mixing process at the outlet of the air heater. To reduce the generated turbulence intensity a honey-comb flow straightener is positioned upstream the measurement section. Due to the limited available space, the turbulence grid as well as the flow straightener are not shown in Fig. 1. Positioned 1.6 m behind the air heater, the square shaped inlet of the measurement section has a side length of 0.4 m and houses a flat plate made of *NECURON* 1007 with an axial chord length of 1m. The flat plate is designed with an elliptic nose as well as an elliptic trailing edge. In case of backflow, as a result of the high amplitude pulsating pressure fluctuations, a straight trailing edge would be unfavorable. A set of five 777-shaped film cooling holes with a lateral spacing of 45 mm is integrated into the plate. The design is related to experimental investigations by Schroeder and Thole [15], who developed a fan-shaped outlet for film cooling holes. The lateral spacing of $c_{lat}/D = 6$ is chosen to focus on periodicity rather than on forcing a uniting of the discrete film cooling flows.

The hole geometry parameters are listed and visualized in the Table 1 and Fig. 2 respectively.

Table 1. 777-hole geometry

Name	Parameter	Value
Injection angle	α	30°
Laidback angle	β_{fwd}	7°
Lateral angle	β_{lat}	7°
Hole diameter	D	7, 5 mm
Lateral hole spacing	c_{lat}	45 mm
Axial position of cooling hole	l_{ax}	38 mm

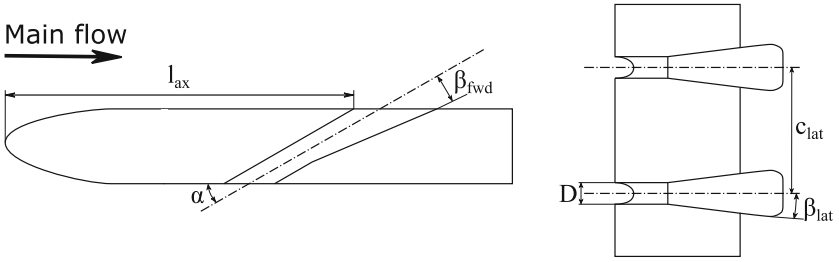

Fig. 2. 777-hole geometry (adapted from Schroeder and Thole [15])

Cooling air for the experiments is provided by an external compressor. The air is dried and cooled before it is stored in a styrofoam-isolated distribution tank from which every cooling hole is fed separately. Besides the flow distribution the tank serves as a damping volume for experiments under pulsating flow conditions. Without this volume the pressure fluctuations would disturb the mass flow controller, which is used to set the desired blowing ratio between the main and secondary air flow. For investigations under periodic unsteady flow conditions a rotating metal disk driven by an electric motor is used. Since the speed of sound at given flow conditions is an order of magnitude larger than the actual main flow velocity the position of the pulse generator will not affect the results of the experimental investigations.

3 Methods

All experiments were performed with a main flow velocity V_∞ of 10 m/s, which corresponds to a mean Reynolds number based on l_{ax} of $Re = 2.2 \times 10^5$ and with a freestream turbulence intensity of $Tu = 5.27\%$. For the determination of the Reynolds number the distance from the leading edge to the cooling hole (l_{ax}) is used (see Fig. 2). The velocity measurement is done via a Prandtl probe with an integrated temperature sensor mounted upstream the flat plate. Due to high blockage under unsteady boundary conditions backflow may occur. Therefore, a second Prandtl probe, directing in the opposite direction of the main flow, is installed downstream the flat plate. In addition, further temperature and total pressure probes are installed inside the nose and the trailing edge of the plate. Pressure data is recorded using *First Sensor* HDO pressure sensors with a 5 mbar pressure range. The length of the pressure tubing is kept to a very minimum and thermocouples are chosen over pt100 temperature sensors. In this way the main flow parameters, e.g. the density ρ_∞, can be characterized even under highly unsteady boundary conditions.

As described in Sect. 2 the periodic pressure fluctuations are produced with a rotating metal disk. With different sized disks pressure amplitudes from 2% to 100% of the mean differential pressure are achievable. The investigated pulse frequencies f_p range from 1 Hz to 5 Hz. For example Fig. 3 shows the main velocity and the total pressure fluctuations during five periods at a pulse frequency of 1 Hz.

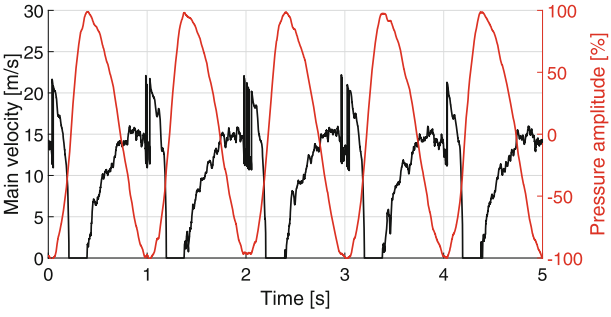

Fig. 3. Velocity and pressure fluctuations during unsteady experiments at 1 Hz

The secondary airflow velocity is controlled by a *Omega FMA 2621A* mass flow controller. For air temperature measurement a PT100-probe inside the distribution tank as well as two Type-K thermocouples inside the outer film cooling holes are used. The mass flow controller, which is connected with the measurement computer, provides necessary data to calculate the density ρ_c and the flow velocity V_c of the cooling flow. Further Type-K thermocouples are flush mounted to the flat plate surface and inserted into the flat plate body to ensure a homogeneous heating of the test specimen prior to each measurement and to also verify the measured temperature of the infrared camera. To characterize the cooling mechanism in a gas turbine, the density ratio between the hot gas from the combustion chamber and the coolant flow extracted from the compressor is used. In modern gas turbines the density ratio ranges up to 1.8 at a pressure ratio between coolant and main flow of 1.02 [12]. The low pressure ratio means, that the density ratio is only driven by the temperature of the cooling flow. Whereas other researchers used different gases to generate a density ratio without a high temperature ratio, the authors in this publication used ambient air for the main and secondary flow due to a long operation time of the wind tunnel to reach a thermal steady state. Therefore only a low density ratio (DR) of 1.1 can be investigated. Nevertheless a comparison to other experimental studies [13,15] is still possible for a smaller range of blowing ratios. As mentioned above the blowing ratio has a high impact on the flow topology. In order to keep the pressure ratio low, as in real gas turbines, only blowing ratios (M) from 0.5 to 1.5 are investigated. The variation of the blowing ratio in that range does not affect the density ratio which was intended by the authors.

The density ratio and the blowing ratio are defined as:

$$DR = \frac{\rho_c}{\rho_\infty} \qquad M = \frac{\rho_c V_c}{\rho_\infty V_\infty}.$$

As mentioned before an infrared thermography system (VarioCam HD 600) from *Infratec* with a resolution of 640×480 pixels at a sampling rate of 30 Hz is used for adiabatic film cooling measurements. This allows to record the desired surface on the flat plate in a single shot with a resolution of 0.3 mm/Px. A lens correction is applied to correct non-uniformity due to the lens curvature. The temperature resolution of 0.05 K is achieved through a manufacturer calibration for the desired temperature range and checked with two flush mounted thermocouples. The *NECURON 1007* material of the flat plate is chosen due to its mat and non-reflecting surface. A logical trigger chain synchronizes the camera sampling rate with the sampling rate of the measurement system and it sets the measurement starting point depending on the position of the rotating metal disk.

In order to set the boundary conditions for the measurement campaign, the temperature of the main flow, the secondary air mass flow and the rotating frequency of the metal disk are adjusted in a closed-loop manner to meet the desired conditions. A *Dewetron 50 PCI* measurement system is used to record the data with a sampling rate of 10.000 Hz.

Table 2. Experimental conditions

Name	Parameter	Value
Main flow velocity	V_∞	10 m/s
Main flow temperature	T_∞	298–323 K
Cooling flow temperature	T_c	290 K
Pulse frequencies	f_p	1–5 Hz
Jet Reynolds number	Re_D	2200–7200

Each measurement point is recorded over five seconds, after the surface temperature of the flat plate reaches a steady state. A full overview of the experimental conditions is given in Table 2.

4 Results

This chapter shows the results of the adiabatic film cooling measurements under steady and unsteady boundary conditions. The measured temperatures will be used to calculate the adiabatic film cooling effectiveness η, which is defined as:

$$\eta = \frac{T_\infty - T_{aw}}{T_\infty - T_c}.$$

Due to the periodicity of the surface visualization, the line plots refer to the middle of the five cooling holes.

Steady Measurements

The investigations under steady conditions serve as a baseline for the unsteady experiments. Furthermore the results allow a comparison to the results from Schroeder and Thole [15]. The surface visualization of the adiabatic film cooling effectiveness η for different blowing ratios M can be seen in Fig. 4. The displayed effectiveness upstream the cooling holes results from heat conduction inside the film cooling holes. Due to a low density ratio DR of 1.1 and a relative high freestream turbulence intensity of 5.27%, the effectiveness distribution downstream of the cooling holes behaves similar for all investigated blowing ratios. The highest film cooling effectiveness with the highest spread in lateral and axial direction can be observed at a blowing ratio of 0.75. For blowing ratios above 1.0 a smaller lateral spread of the cooling flow can be detected. This effect results of strong counter-rotating vortex pairs as described by Ostermann et al. [11].

There is a small skewness in lateral distribution for low blowing ratios detectable. The authors believe, that the air heater, which is located upstream the measurement section, creates an inhomogeneous flow field. The chosen spacing between the turbulence grid and the flow straightener seems not sufficient for a complete mixing process. In addition a little difference in the supply for

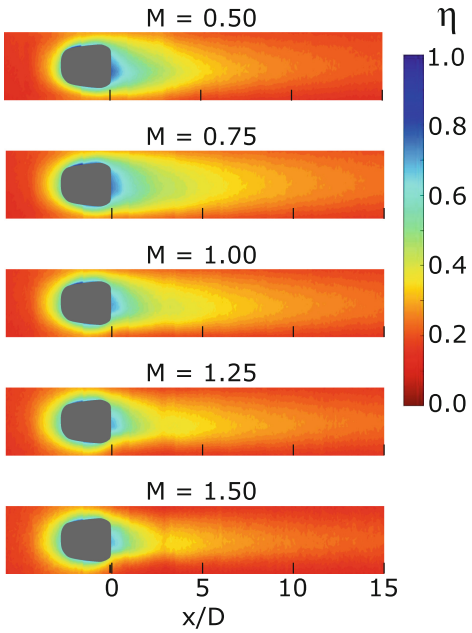

Fig. 4. Adiabatic film cooling effectiveness under steady inflow conditions

the film cooling holes can also result in an uneven lateral distribution of film cooling effectiveness.

Figure 5 shows the adiabatic effectiveness along the centre line of the middle film cooling hole for a normalized axial distance x/D of 15. Additional experimental data from Schroeder and Thole [15] is included. The centre line data from Schroeder and Thole was measured with a density ratio of 1.5 and a freestream turbulence intensity of 0.5. These setup differences are the reason for the lower cooling performance within the presented study, especially the turbulence intensity is a major factor as observed by Saumweber et al. [13].

Nevertheless the results for low blowing ratios are similar to those for low blowing ratios from Schroeder and Thole. The lower the blowing ratio, the better is the adiabatic effectiveness - except for a ratio of M = 0.5. It shows best results in the near field, but the mass flow is just not sufficient to maintain the protective shield for values x/D > 5. All blowing ratios indicate a steep negative gradient over an axial distance from 0 to 4 x/D with. For higher blowing ratios > 1.00 a saddle point between 5 and 6 x/D can be detected. This behavior can be explained with a reattached cooling flow.

The lateral distribution at a fixed axial position (x/D = 5) is illustrated in Fig. 6. As seen in Fig. 4 the lateral spread of the cooling film for blowing ratios above 1.0 is smaller than for low blowing ratios. The lateral distribution for a blowing ratio of 1.0 at a high density ratio from Schroeder and Thole is displayed as well. The maximum film cooling effectiveness in the centre is significantly

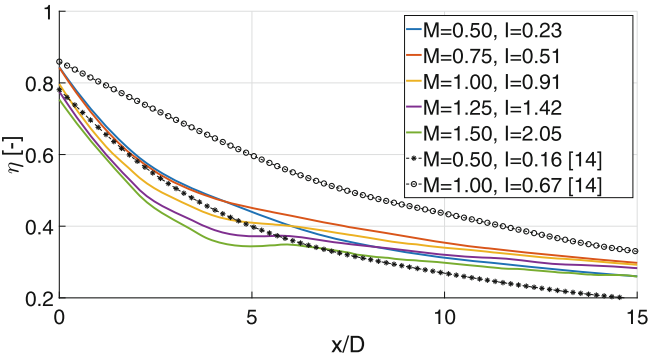

Fig. 5. Adiabatic film cooling effectiveness along the centre line of a film cooling hole

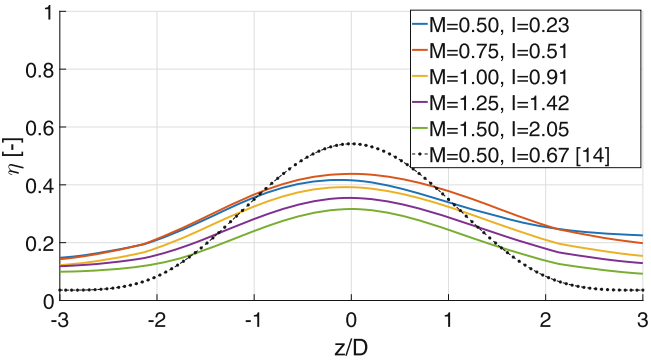

Fig. 6. Lateral distribution of film cooling effectiveness at x/D = 5

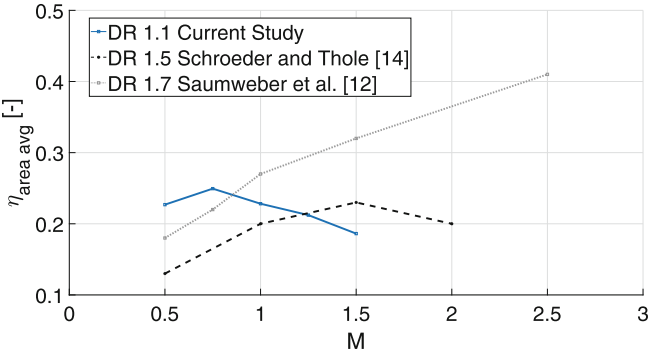

Fig. 7. Area-averaged film cooling effectiveness over x/D = 2–22

larger compared to the evaluated blowing ratios in this study. However, the lateral spread for the blowing ratio of 1.0 is similar in both studies.

In Fig. 7 the area-averaged film cooling effectiveness is compared to other film cooling investigations. As also observed by Schroeder and Thole, who investigated two different density ratios, the maximum area-averaged effectiveness is shifted to lower blowing ratios as a result of the lower density ratios [15].

Saumweber et al. investigated fan-shaped film cooling holes with a reduced injection angle α and a higher density ratio of 1.7. Due to this setup there is no maximum in effectiveness reached within a blowing ratio range from 0.5 to 2.5.

In conclusion, the overall cooling performance under steady conditions depends, besides the blowing ratio, highly on the density ratio and the turbulence intensity. The evaluation of measured data and the comparison of film cooling effectiveness with data from literature proves the usability of the setup. Referring to the steady measurements, the results of the experiments under unsteady boundary conditions will be presented in the following chapter.

Unsteady Measurements

The unsteady measurements were performed for different pressure amplitudes with different sized metal disks for periodic blockage. However, only the largest metal disk could produce significant periodic pressure amplitudes to mimic a pressure gain combustion concept. Therefore the evaluation of unsteady measurement data refers only to experiments with a pressure amplitude of 100% to the mean differential pressure (see Fig. 3). The highly unsteady character of the main flow field affects the secondary air flow path as well. The main control parameter, e.g. blowing ratio, secondary air flow pressure and cooling air density are fluctuating also in a wide range. Therefore, only blowing ratios up to 1.0 are evaluable for a density ratio of 1.1.

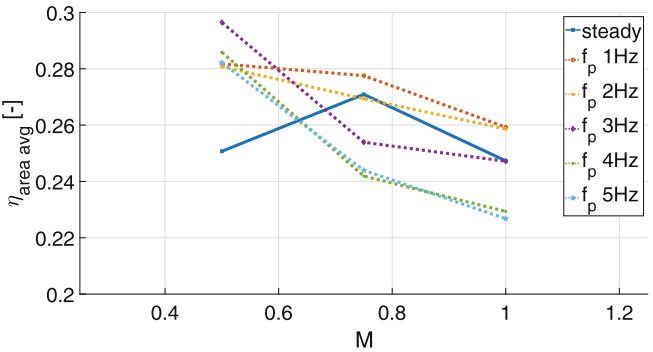

Fig. 8. Area- and time-averaged film cooling effectiveness over x/D = 0–20 for different pulse frequencies under periodic pressure amplitude of 100%

Figure 8 shows the area- and time-averaged film cooling effectiveness for different pulse frequencies f_p and blowing ratios M. The steady measurement data

is also included for a better comparison of the different boundary conditions. The trend of the steady measurement with a peak effectiveness at a blowing ratio of 0.75 does not apply for a main flow with periodic pressure fluctuations. For all investigated frequencies a low blowing ratio seems beneficial for a higher cooling effectiveness compared to the steady case. With an increasing blowing ratio the area-averaged effectiveness decreases for all investigated pulse frequencies. Compared to the steady case, low frequencies from 1 Hz to 2 Hz produce better or equal time-averaged cooling effectivenesses for all investigated blowing ratios. The evaluation of higher pulse frequencies results in a steeper negative gradient with increased blowing ratio. Under the influence of higher frequencies (>3 Hz) of pressure fluctuations the area-averaged cooling effectiveness is reduced by a maximum of 11% for the blowing ratios 0.75 and 1.00.

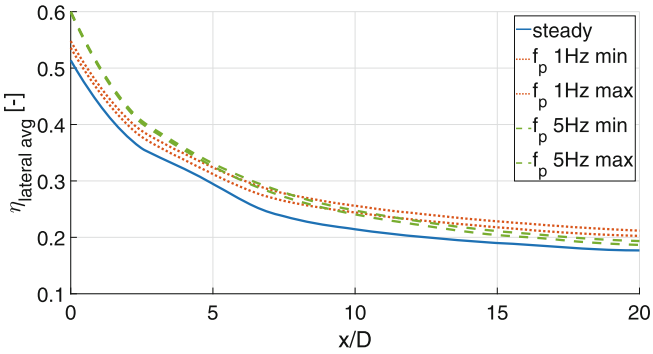

(a) Blowing ratio 0.5

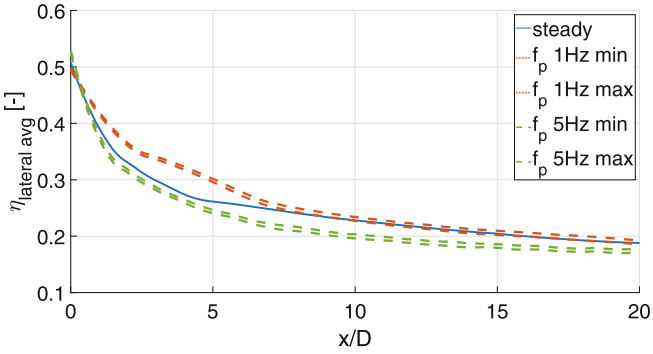

(b) Blowing ratio 1.0

Fig. 9. Minimum and maximum lateral-averaged film cooling effectiveness for pulse frequencies 1 Hz and 5 Hz

Figure 9 shows the lateral-averaged film cooling effectiveness over a distance x/D of 20. In both figures the steady baseline and the pulse frequencies 1 Hz and 5 Hz are compared. In addition, for each frequency the minimum and maximum lateral-averaged film cooling effectiveness over one pulse period is shown. For a

blowing ratio of 0.5 (see Fig. 9a) the lateral-averaged effectiveness is increased for both unsteady cases. At the first half of the investigated distance a higher pulse frequency seems beneficial, whereas a pulse frequency of 1 Hz produce an increased lateral averaged cooling effectiveness above a distance x/D of 10. In both Figs. 9a and 9b the spread between minimum and maximum film cooling effectiveness increases along the axial distance for all experiments under the influence of periodic pressure fluctuations. This effect will cause fluctuating high thermal loads downstream the cooling holes which can influence the lifetime of the turbine negatively. Therefore a detailed investigation of the downstream area x/D above 20 is highly recommended for further experiments.

For a blowing ratio of 1.0 only a low pulse frequency results in a higher lateral-averaged cooling effectiveness, which can be seen in Fig. 9b. Especially over a distance x/D from 1 to 6 a significant rise in effectiveness is observable. This behavior can be explained by the slow rotation of the pressure pulse generating metal disk. The acceleration and deceleration of the wind tunnel over one pulse period takes more time for low frequencies than for high frequencies. During this unsteady process the secondary air flow is able to generate a higher heat transfer during phases of periodic acceleration and deceleration. According to Fig. 3 the peak of the main velocity reaches 20 m/s and during a short time of the pulse period the flow velocity is 0 m/s. Due to the strong main velocity fluctuations the blowing ratio changes periodically as well. The time-averaged blowing ratio is 1.02 but the time-resolved values alternates between 0.5 and 6.5 mainly. Compared to the steady baseline there are time steps during one pulse period, in which the blowing ratio leads to an attached flow.

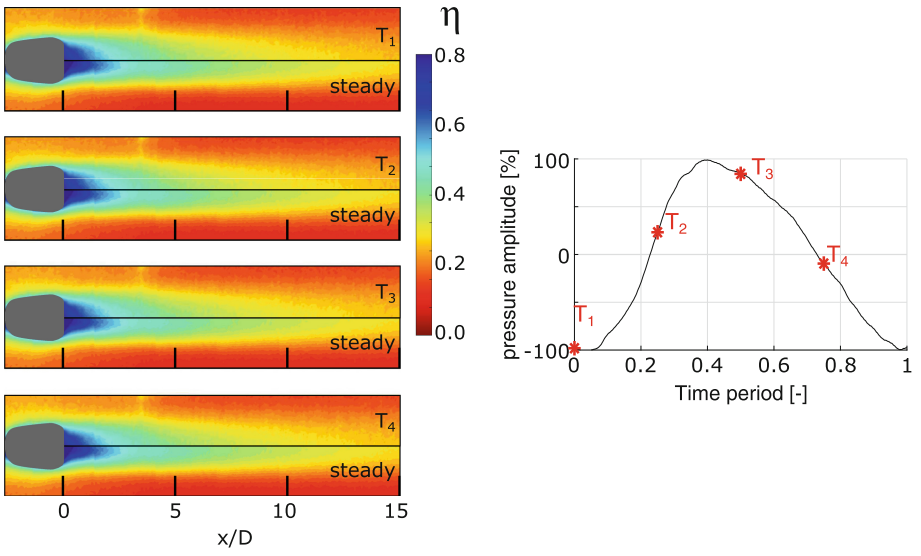

Fig. 10. Time-resolved field of adiabatic film cooling effectiveness with a blowing ratio of 1.0 and a pulse frequency of 1 Hz

A time-resolved field of the adiabatic film cooling effectiveness at specific points of time over an entire period is presented in Fig. 10. The steady measurement is inserted in the lower half of the effectiveness field to allow for comparison. The time steps are equally quartered over a full pulse period T. Compared to the lower half of each time step the lateral spread is larger under periodic pressure fluctuations, as seen in Fig. 9b. However, the axial expansion of the cooling flow under steady conditions is larger by almost 33%. This effect has to take into account for an arrangement of cooling holes under the influence of pressure fluctuations caused by a pressure gain combustion. All four time frames show that there is no constriction of cooling effectiveness at the outlet of the fan-shaped hole. The periodic fluctuating main flow seems to be the reason for a better distribution of the cooling flow at higher blowing ratios.

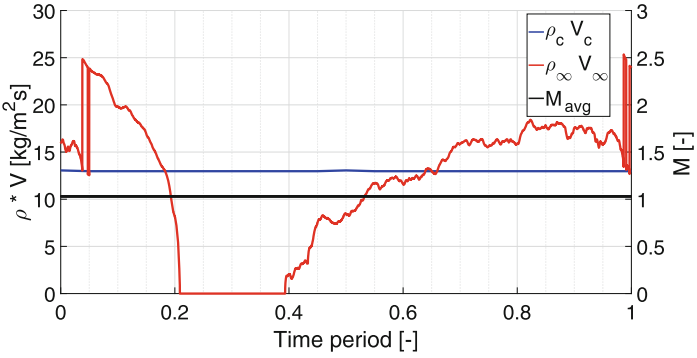

Fig. 11. Time-resolved blowing ratio for a pulse frequency of 1 Hz

Referring to the evaluation in Fig. 10, Fig. 11 shows the time-resolved blowing ratio which is phase-averaged over five pulse periods. The time-averaged blowing ratio is displayed as well. The used coolant mass flow is equal for steady and unsteady investigations as long as the time-averaged blowing ratio and the density ratio is kept constant during the investigations. As a result of the high blockage and the pressure wave, the main flow velocity experiences its minimum which results in the peak in blowing ratio at time point 0.4 s (due to $M = \rho_c V_c / \rho_\infty V_\infty$). A detached flow during this short period of time can be assumed. This effect and the impact on film cooling effectiveness needs to be investigated in further experiments. Future experiments will additionally be carried out at the Hot-Acoustic-Testrig (HAT) which allows for engine realistic conditions. Also the development of control algorithms for an adapted blowing ratio depending on the pulse frequency and pressure amplitude is conceivable.

5 Conclusion

In this contribution the adiabatic film cooling effectiveness for a set of 777 fan-shaped cooling holes under the influence of pulsating inflow conditions is analyzed. First, fundamental steady measurements were performed and compared to results from literature. Due to a low density ratio of 1.1 and a high turbulence intensity of 5.27% a peak effectiveness at a blowing ratio of 0.75 could be evaluated.

In a further step, the influence of periodic pressure fluctuations on the area-averaged film cooling effectiveness is analyzed. Although this investigation has only considered isolated cooling holes on a flat plate, neglecting induced pressure gradients resulting from real geometry blade curvatures, a few conclusions can be carefully drawn:

- An influence of the pressure waves on the film cooling effectiveness field was shown with the time-resolved analysis.
- The periodic fluctuating main flow velocity is beneficial for lower blowing ratios over all investigated pulse frequencies f_p.
- With increasing blowing ratios only frequencies from 1 Hz to 2 Hz result in a similar or an even better area-averaged cooling performance (as was also stated by Womack [21]).
- The lateral displacement of the cooling film is slightly increased.
- However, the axial expansion is reduced especially for higher pulsating frequencies.

Figure 12 summarizes the findings of this publication in a heat map, highlighting the beneficial areas. Following the question for the overall cooling requirement the authors conclude an increased demand in cooling air. The decreased axial expansion demands a new array of cooling holes to be positioned further upstream thus increasing the number of cooling holes which increases the cooling air demand. Further, higher frequencies of the pulsating inflow conditions actually induce a new steady state. In this condition the cooling film has no time to recover. In order to ensure a sufficient blade protection, the cooling air supply has to be adjusted to the new back pressure resulting in a higher demand. Last but not least, the investigations using the TU-Pulse testrig [7] have shown a movement of the stagnation line on the NGV. As a consequence, the vulnerable temperature peak area is increased which calls for an increase of the film cooling area thus again demand more cooling mass flow.

In summary, these results represent a basic set of measurement data for film cooling effectiveness of fan-shaped under the influence of high amplitude inflow conditions. Further investigations with higher density ratios and a wider range of blowing ratios are recommended. Especially a quantification of the increased cooling air mass flow is necessary in order to derive possible counter measures.

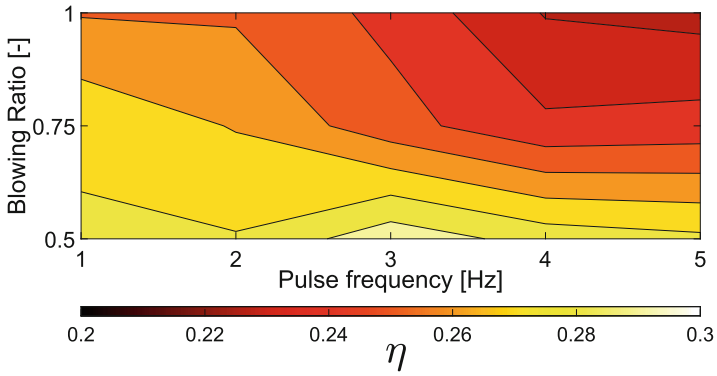

Fig. 12. Surface plot of adiabatic film cooling effectiveness compared to investigated parameters for unsteady main flow

Acknowledgements. The authors acknowledge the support for this research by the Deutsche Forschungsgemeinschaft (DFG) in the context of the Collaborative Research Center CRC1029 'Substantial Efficiency Increase in Gas Turbines through Direct Use of Coupled Unsteady Combustion and Flow' through sub-project B05.

References

1. Baheri, S., Tabrizi, S.P.A., Jubran, B.A.: Film cooling effectiveness from trenched shaped and compound holes. Heat Mass Transf. **44**(8), 989–998 (2008). https://doi.org/10.1007/s00231-007-0341-9
2. Bakhtiari, F., Schiffer, H.P.: Numerical investigation of film cooling effects under transient inflow. In: 24th International Symposium on Air Breathing Engines (2019)
3. Bunker, R.S.: A review of shaped hole turbine film-cooling technology. J. Heat Transf. **127**(4), 441 (2005). https://doi.org/10.1115/1.1860562
4. Dähnert, J., Lyko, C., Peitsch, D.: Transition mechanisms in laminar separated flow under simulated low pressure turbine aerofoil conditions. J. Turbomach. **135**(1), 011007 (2012). https://doi.org/10.1115/1.4006393
5. Deinert, M., Hourmouziadis, J.: Film cooling in unsteady flow with separation bubble. In: Volume 3: Turbo Expo 2004, pp. 55–66. ASMEDC (2004). https://doi.org/10.1115/GT2004-53075
6. Heidmann, J.D., Lucci, B.L., Reshotko, E.: An experimental study of the effect of wake passing on turbine blade film cooling. J. Turbomach. **123**(2), 214 (2001). https://doi.org/10.1115/1.1354621
7. Heinrich, A., Herbig, M., Peitsch, D., Topalovic, D., King, R.: A testrig to evaluate turbine performance and operational strategies under pulsating inflow conditions. In: AIAA Propulsion and Energy 2019 Forum. American Institute of Aeronautics and Astronautics (2019). https://doi.org/10.2514/6.2019-4039
8. auf dem Kampe, T., et al.: Experimental and numerical investigation of flow field and downstream surface temperatures of cylindrical and diffuser shaped film cooling holes. In: Volume 5: Heat Transfer, Parts A and B, pp. 21–34. ASMEDC (2011). https://doi.org/10.1115/GT2011-45106

9. Lyko, C., Dähnert, J., Peitsch, D.: Forcing of separation bubbles by main flow unsteadiness or pulsed vortex generating jets - a comparison. J. Turbomach. **136**(5), 051016 (2013). https://doi.org/10.1115/1.4025214
10. Neumann, N., Peitsch, D.: A comparison of steady-state models for pressure gain combustion in gas turbine performance simulation (accepted for publication). In: Proceedings of GPPS Beijing 2019. GPPS-BJ-2019-0198 (2019)
11. Ostermann, F., Woszidlo, R., Nayeri, C., Paschereit, C.O.: The time-resolved flow field of a jet emitted by a fluidic oscillator into a crossflow. In: 54th AIAA Aerospace Sciences Meeting (2016). https://doi.org/10.2514/6.2016-0345
12. Sargison, J.E., Guo, S.M., Oldfield, M.L.G., Lock, G.D., Rawlinson, A.J.: A converging slot-hole film-cooling geometry–part 2: transonic nozzle guide vane heat transfer and loss. J. Turbomach. **124**(3), 461–471 (2002). https://doi.org/10.1115/1.1459736
13. Saumweber, C., Schulz, A., Wittig, S.: Free-stream turbulence effects on film cooling with shaped holes. J. Turbomach. **125**(1), 65–73 (2003). https://doi.org/10.1115/1.1515336
14. Schroeder, R.P.: Influence of in-hole roughness and high freestream turbulence on film cooling from a shaped hole. Ph.D. thesis, The Pennsylvania State University (2015)
15. Schroeder, R.P., Thole, K.A.: Adiabatic effectiveness measurements for a baseline shaped film cooling hole. In: Proceedings of ASME Turbo Expo 2014: Turbomachinery Technical Conference and Exposition, Düsseldorf, Germany, p. V05BT13A036 (2014). https://doi.org/10.1115/GT2014-25992
16. Schroeder, R.P., Thole, K.A.: Effect of high freestream turbulence on flowfields of shaped film cooling holes. J. Turbomach. **138**(9), 091,001-1–091,001-10 (2016). https://doi.org/10.1115/1.4032736
17. Schroeder, R.P., Thole, K.A.: Effect of in-hole roughness on film cooling from a shaped hole. J. Turbomach. **139**(3), 031,004-1–031,004-9 (2016). https://doi.org/10.1115/1.4034847
18. Schroeder, R.P., Thole, K.A.: Thermal field measurements for a shaped hole at low and high freestream turbulence intensity. J. Turbomach. **139**(2), 021,012-1–021,012-9 (2016). https://doi.org/10.1115/1.4034798
19. Stathopoulos, P.: Comprehensive thermodynamic analysis of the humphrey cycle for gas turbines with pressure gain combustion. Energies **11**(12), 3521 (2018). https://doi.org/10.3390/en11123521
20. Topalovic, D., Wolff, S., Heinrich, A., Peitsch, D., King, R.: Minimization of pressure fluctuations in an axial turbine stage under periodic inflow conditions. In: AIAA Propulsion and Energy 2019 Forum. American Institute of Aeronautics and Astronautics (2019). https://doi.org/10.2514/6.2019-4213
21. Womack, K.M., Volino, R.J., Schultz, M.P.: Measurements in film cooling flows with periodic wakes. J. Turbomach. **130**(4), 041008 (2008). https://doi.org/10.1115/1.2812334